Available online at www.sciencedirect.com
ScienceDirect
Journal of the European Ceramic Society 27 (2007) 1411–1417
www.elsevier.com/locate/jeurceramsoc

Friction behavior of sintered metallic brake pads on a C/C–SiC composite brake disc

Zmago Stadler [a], Kristoffer Krnel [b,*], Tomaz Kosmac [b]

[a] *MS Production, Pot na lisice 17, Bled, Slovenia*
[b] *Jozef Stefan Institute, Jamova 39, Ljubljana, Slovenia*

Available online 24 May 2006

Abstract

In this study we report on the frictional and wear properties of sintered metallic (MMC) brake linings in combination with a C/C–SiC brake disc. The influence of additives, such as graphite, and abrasives in the metallic matrix on the formation of the friction layer was investigated using a scanning electron microscope (SEM) equipped with energy-dispersive X-ray spectroscopy (EDX) and Auger electron spectroscopy (AES). The formation of a friction layer on the pad's worn surface consisting mostly of iron and copper oxides was confirmed. The frictional properties of the sintered metallic brake pads were determined and related to the composition and structure of the friction layer. This investigation of the friction characteristics of a brake couple comprising (MMC) brake linings and a C/C–SiC composite disc will increase the understanding of this material, which from the tribological point of view works in a completely different way than a classical disc brake based on gray cast-iron.

Keywords: Carbon; SiC; Composites; Friction properties

1. Introduction

The potential for using carbon/carbon (C/C) materials in brake discs and pads has been known for a relatively long time.[1] Brake systems using these materials were first introduced in aircraft, and then later in racing cars and motorcycles. However, these systems still suffered some disadvantages, such as a low coefficient of friction at temperatures below 450 °C and a high rate of wear for the pads. Therefore, a short-fibre-reinforced SiC material (C/SiC) was developed for lightweight brake discs to be used in sports cars and high-speed trains.[2,3]

More recently, a novel type of C/C–SiC brake disc has been developed; this disc consists of a woven-carbon-reinforced carbon-core material and a thin surface layer of SiC.[4] The friction properties of this disc material, which was specially developed for friction applications such as brake discs and clutch facings, are much better than those of conventional C/C composite materials. Furthermore, the material exhibits good corrosion and oxidation resistance and excellent wear properties. As shown in Fig. 1, this material consists of a C/C core with a thin silicon-carbide coating. The manufacturing process involves the preparation of a supporting 2D C/C composite core of the desired geometry, which is then subjected to a liquid-silicon-infiltration (LSI) process in a high-temperature furnace under vacuum.[5,6] The reaction-bonded SiC layer is formed on the surface of the C/C core, resulting in good resistance to corrosion and oxidation. The final operation is the surface grinding of the sliding surfaces on the disc.

Since extremely high temperatures are generated on the disc surfaces during braking, tribologically matching brake pads need to be developed, and the brake caliper needs to be redesigned to protect it from the high temperatures generated on the disc surface during braking.[7]

In order to find matching brake pads various composite materials were tested as the brake linings in combination with the C/C–SiC brake disc.[7] The brake pads represent the replaceable element in the friction couple and are typically rubbed against the brake disc. The friction behavior of classical brakes (organic brake pads/gray cast-iron or steel brake discs) is determined by the character of the brake surfaces of the disc and pad and by the friction layer between these surfaces. The formation of this friction layer on friction surfaces is very complex and variable, and it remains incompletely explored and poorly understood.[8–10]

Here we report on an investigation of the friction characteristics of a brake couple composed of a sintered brake lining (MMC) and a C/C–SiC composite disc. From the tribological

* Corresponding author. Tel.: +386 1 4773784; fax: +386 1 4263126.
E-mail address: kristof.krnel@ijs.si (K. Krnel).

0955-2219/$ – see front matter © 2006 Elsevier Ltd. All rights reserved.
doi:10.1016/j.jeurceramsoc.2006.04.032

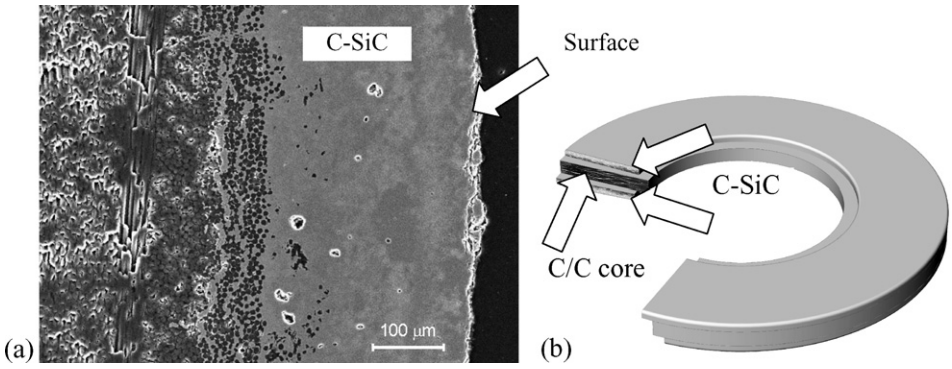

Fig. 1. Structure of the composite brake disc: (a) SEM micrograph of the SiC layer on the C/C composite base and (b) schematic representation of the composite disc.

point of view such a couple works in a completely different way than a classical couple braking on a gray cast-iron disc. However, there is a lack of publications in this field, which is probably due to the fact that any analysis and characterization of the brake pad surface are difficult because of the heterogenic composition of the pad, the mechanical and chemical interactions occurring in the friction process and the repeatability of the testing conditions during friction-performance testing.

The objective of this present study was to investigate the influence of the constituents, such as graphite and SiC, on the friction, mechanical and tribochemical characteristics of the base metallic matrix of the pad.

2. Experimental

2.1. Composition of the brake pads

The lining material of sintered brake pads usually consists of different base metal powders (iron, copper, copper alloys or a mixture of these) and frictional additives (abrasives, solid lubricants).

A special formulation (Table 1) was designed for the brake friction couple operating on the C/C–SiC disc. For the base metallic matrix we used commercial atomized metal powders: copper, with an average particle size below 80 μm; bronze CuSn10, with an average particle size below 355 μm, from Pometon, Italy; iron powder, with an average particle size below 212 μm, from Högenäs, Sweden; steel powder alloyed with Cr, Mo, V and W carbides, with an average particle size below 100 μm, from Högenäs, Great Britain. For the frictional additives we used SiC powder with an average particle size of 10–15 μm, Saint Gobain, France; synthetic graphite powder with an average particle size of 150–600 μm, Timcal, Switzerland. The mixed powders where consolidated into a lining on a copper-plated steel back-plate by die compaction at 400 MPa at room temperature. The dry-pressed brake pads were than sintered for 1 h at 970 °C under a N_2 (3% H_2) atmosphere. The sintered brake pads were then ground to a proper thickness for the testing of their friction properties. The brake contact area was 10.2 cm^2.

Table 1
Formulation of the investigated brake-lining materials (wt.%)

Constituents	M35[a]	G15	K5
Copper powder	54	46	52
Iron powder	25	21	24
Steel powder (HSS)	15	13	14
Bronze powder	6	4	5
Graphite		15	
SiC			5

[a] M35—the base metallic matrix composition was constant in all the investigated formulations.[15]

2.2. Friction and wear test

The friction and wear properties of the couple consisting of the sintered brake pads and the C/C–SiC composite disc were evaluated with dynamometer (Krauss RWS 75B, Germany) testing according to ECE R90, Annex. 8.[11] The brake system consisted of a redesigned commercial rear caliper (Brembo, Bergamo, Italy) and a ceramic composite disc of Ø196 mm × 6 mm with an effective radius of 84.5 mm (MS Production, Bled, Slovenia). The specific pressure was 1.14 MPa, whereas the hydraulic pressure was 1.48 MPa. The speed was held constant at 660 min^{-1}.

2.3. Microhardness measurement

The Vickers microhardness of the sintered metallic phases in the base matrix was measured on microhardness testing apparatus (Fischerscope HM2000, Germany) applying a load of 50 mN. Ten measurements were made of each phase on a polished perpendicular section.

2.4. Characterization of the friction surface

The friction surfaces before and after the test and the developed friction layer were all analyzed using a scanning electron microscope (JSM-5800, Jeol, Japan) equipped with a Link energy-dispersive X-ray analyzer (EDX). Some of the surfaces were additionally characterized by Auger electron spectroscopy (AES) (PHI SAM Model 545A). During the AES

Table 2
Friction and wear properties of the different pad formulations on the C/C–SiC composite brake disc (μ_{OP} scattered within ±5%)

	M35	G15	K5
μ_{OP}	0.55	0.60	0.50
Specific wear by volume (m^3/MJ)	9.3×10^{-6}	25.6×10^{-6}	41.0×10^{-6}

profile analysis the samples were sputtered with two ion-beam guns (Ar^+, 3 keV, angle of incidence 49°) at a sputtering rate of around 6 nm min^{-1}. The samples for all the observations were carefully cut off from a real-size brake pad in order to avoid any modification of the friction surface. In order to be able to analyze the friction layer in the perpendicular direction with respect to the friction surface, selected samples were deposited with a CrN hard coat, embedded into molding resin and finally ground and polished using standard metallographic procedures.

3. Results and discussion

3.1. Friction and wear properties

The performance of the various investigated materials under the same testing conditions (ECE R90 Annex. 8) is characterized by the coefficient of friction (COF) and the wear rate (Table 2). When comparing the mean COF (μ_{OP}) during a braking test of the M35 sample (only metal constituents) and the formulations with the addition of graphite (G15), we found that the COF increased with a increased graphite content. The addition of the SiC abrasive to the base metallic matrix (K5) resulted in a lower mean COF (Table 2, Fig. 2). This is the opposite of what we expected, and it indicates the chemical and physical changes on the friction surface. The wear of the linings was higher with the addition of graphite and SiC. The addition of graphite tends to make the pads softer, and combined with the higher mean COF increase at the peak temperature of the test (>500 °C) (Fig. 2) this means that the wear of the pad is higher too. The SiC addition increases the hardness of the base metallic matrix, but it also decreases the density of the matrix as a result of poorer sintering. The K5 samples showed increased wear at a much lower peak temperature (450 °C). Comparing the individual friction diagrams in Fig. 2 shows a relatively stable COF versus temperature for the M35 sample, with a steadily increasing COF for the sample with the graphite addition, G15, and an unstable COF for the K5 sample (Fig. 2). In general, practically all the sintered lining formulations had a very low wear rate (ranging from 10 to 25×10^{-6} m^3/MJ).

An increasing COF with the addition of graphite has already been observed for a friction couple composed of a sintered lining combined with a gray cast-iron disc.[12] A tentative explanation was given for these phenomena involving an increase in the friction with an increase in the graphite content that decreases the hardness of the pad: the softer the material, the larger the actual contact area, and so the higher the COF. It seems that this can also apply to the sintered lining and the C/C–SiC discs.

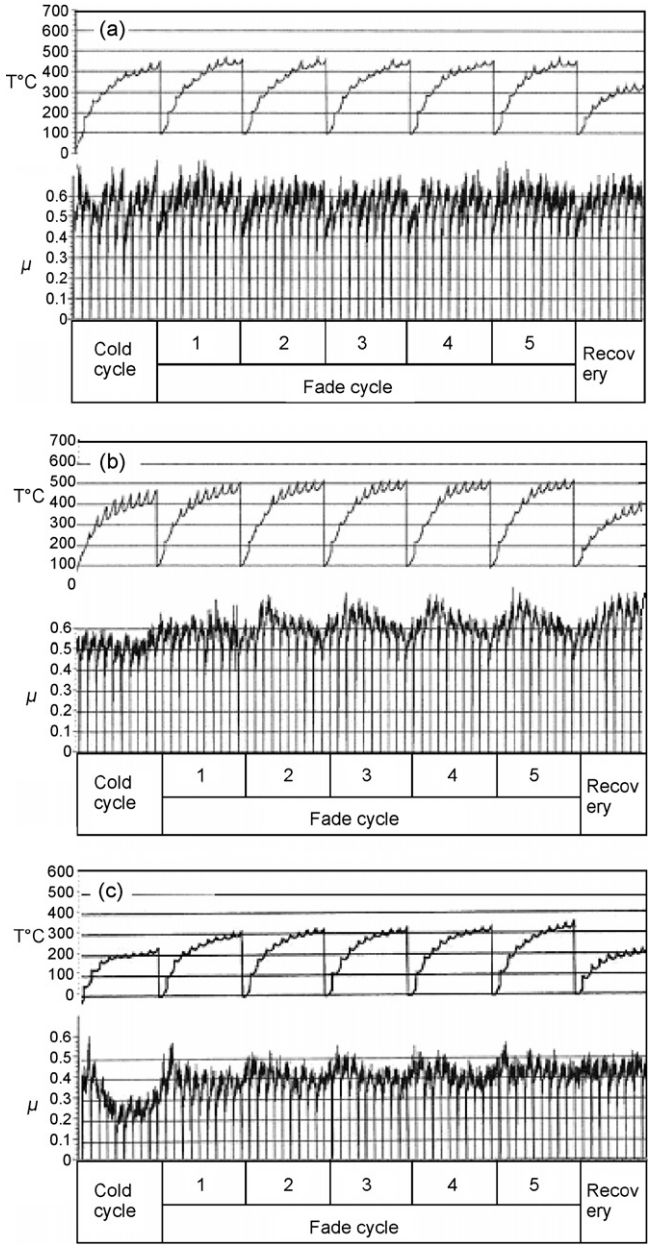

Fig. 2. Friction performance (μ and disc surface temperature) for samples M35 (a), G15 (b) and K5 (c) during braking according to ECE R90 test procedure. Cold, fade and recovery cycles are presented.

3.2. Characterization of the friction surfaces

Due to the very hard and chemically resistant ceramic surface of the brake disc major chemical and physical changes appeared on the brake-pad sliding side.

The friction process is characterized by a modification to the base metallic matrix due to plastic deformation and additional sintering of the sintered metallic constituents, and the development of friction debris that adheres to the friction surface and partially oxidizes forming a friction layer. Together with the

deformed metal phases it forms a friction zone on the sliding surface of the pad (Fig. 3a). It is clear that this area is denser than the inner part of the lining.

The friction layer can be described as a two-layer structure of iron and copper oxides. It is heterogeneous, uneven in its thickness, and with iron oxides as a lower layer and a copper oxides layer on top (Fig. 3c). This friction layer was formed on top of an approximately 30–40-μm-thick mixed metallic zone (Fig. 3b and c) where the original metallic phases are plastically deformed due to the high temperature and the pressure during braking. The highest measured temperature in the contact with the C/C–SiC disc exceeded 500 °C during the braking cycles (Fig. 2a). Based on the high temperature gradient beneath the surface of the pad and taking into account the nature and structure of the C/C–SiC disc, we believe that the actual contact temperature could be as high as 700 °C or more.[13,14]

The AES analyses on the brake-pad friction layer indicated a two-layer oxide structure. The concentration-profile diagrams of samples M35 and G15 (Fig. 4) show that in the case of the M35 sample, below a very thin carbon film there is a copper-rich region. Carbon film is the contamination from disc surface (SiC). The concentrations of O and Fe increase, and at the same time the Cu concentration decreases. Most of the oxygen is combined with iron; the copper is only partially oxidized. The concentration-profile diagram of the G15 sample shows a slightly increased concentration of copper on the top of the friction layer; this is followed by Fe, which is oxidized. Compared to the M35 sample this oxide layer contains more copper and less oxygen because of the lower Fe concentration. In this lining material oxygen is mainly bound to the iron.

The base metallic matrix consists of three phases (Fig. 3b): a copper-based phase (light gray), iron (dark gray) and steel with carbide precipitates (dark gray with white spots). Even when other additives (graphite, abrasives and friction modifiers) are added to the base matrix these three phases are present and the mixed laminar metallic area is formed on top (Fig. 5a). If abrasives are added the mixed metal area is not so well developed, probably because of the higher hardness of the K5 pad material (Fig. 5b).

In order to determine the average hardness of the lining, the microhardnesses of the different metallic phases in the M35 samples were measured (Table 3).

The overall hardness of each formulation can now be calculated as a sum of the microhardness weight by volume fraction by applying the following equation[12]:

$$\mathrm{HV}_{\mathrm{average}} = \sum \mathrm{HV}_n v_n \quad (n = 1 - 5)$$

Table 3
Vickers microhardness of the different phases (load 50 mN)

	Vickers microhardness
The copper-rich phase	143
The iron-rich phase	216
The HSS phase	717

The value of HV 12 was found in Gmelin[16] for the graphite phase. The value of HV 3100 was found in the NIST Property Data Summaries for the SiC particles.

where $\mathrm{HV}_{\mathrm{average}}$ is the average hardness, HV_n the Vickers microhardness of phase n, and v_n is the volume fraction of phase n.

The volume fractions of the main constituent phases, calculated on the basis of actual densities, are given in Table 4.

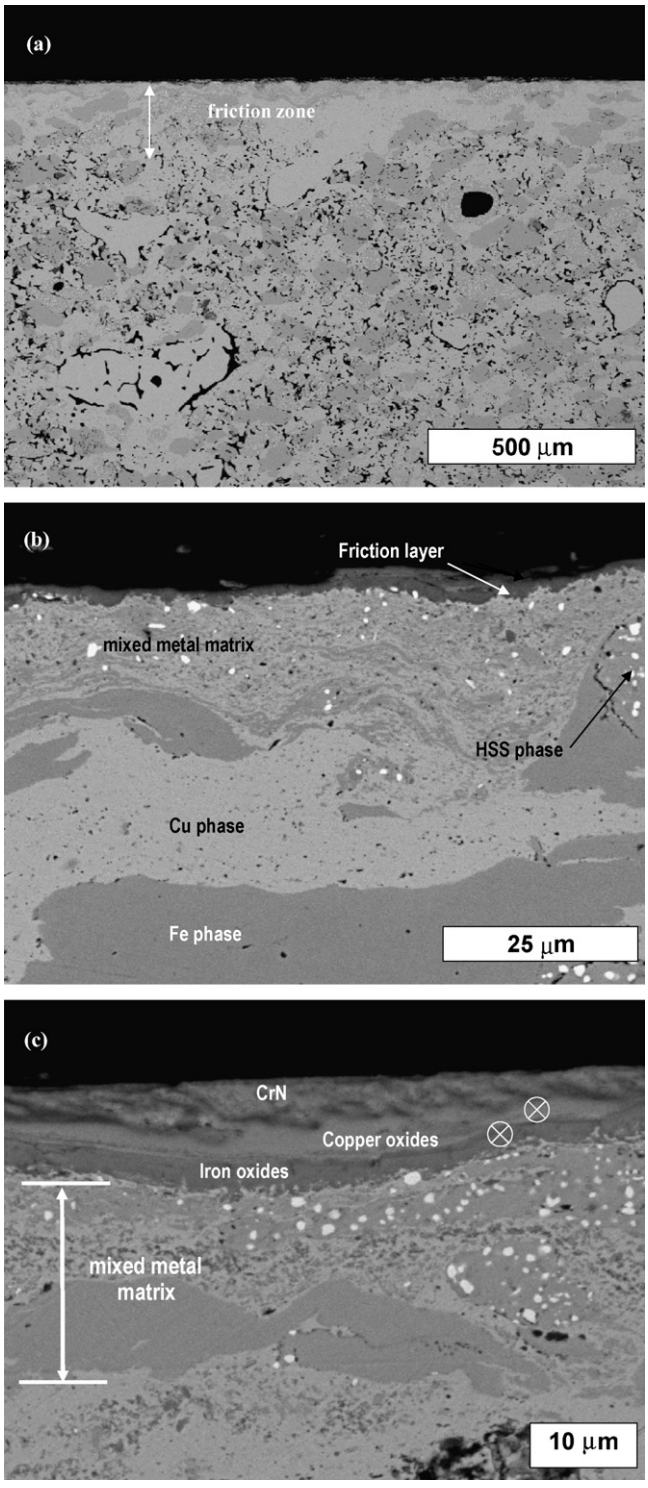

Fig. 3. Friction layer developed on the friction surface of the M35 sample after 100 braking tests. Perpendicular cut with respect to the friction surface: (a) general view demonstrating the denser mixed metallic friction zone, (b) detail from (a) showing laminar mixed area, (c) detail from (b) showing the thickness and structure of the friction layer as shown on the EDX spectra (d).

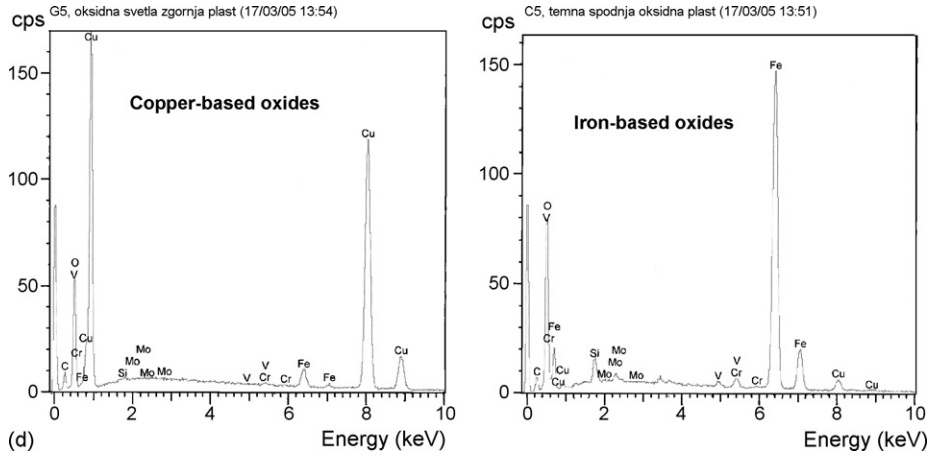

Fig. 3. (*Continued*).

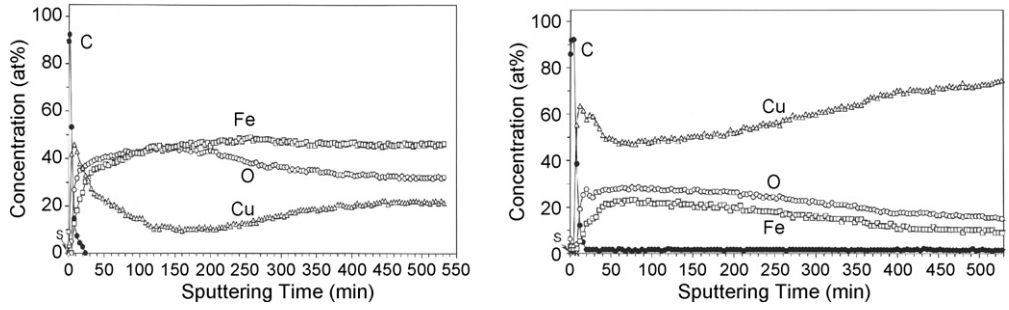

Fig. 4. AES profile analysis diagrams of samples M35 (left) and G15 (right). Sputtering time approximately 9 h, analyzing depth 3 μm.

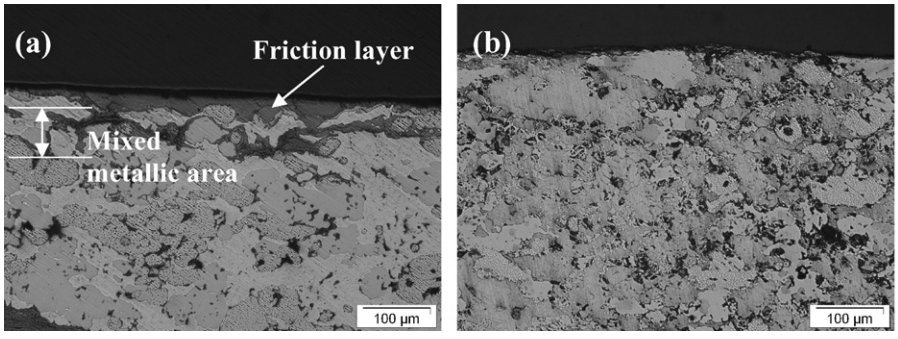

Fig. 5. Microstructure of two pad materials with the addition of graphite (a) (G15) and SiC (b) (K5). The deformation of the base metallic matrix is more clearly visible in the G15 sample than in the K5 sample, where the abrasive particles suppress the moving of the metallic phases.

Table 4
The volume fractions (vol.%) of the copper-rich phase, the iron phase, the HSS phase, the graphite phase, the SiC phase and the porosity

	M35	G15	K5
Copper-rich phase	49.0	28.3	40.9
Iron phase	23.7	13.7	19.7
HSS phase	14.3	8.3	11.9
SiC			10.4
Graphite		35.6	
Porosity	13.0	14.0	17.0

This means that the level of porosity in the materials is included and compared to the concentrations given in Table 1. The volume fractions of the copper-rich phase (copper + bronze), the iron phase, and the HSS phase are given as the initial contents. The volume change that occurs as a result of the interdiffusion between phases is not included in Table 4, except for the copper-rich phase, where the copper and bronze contents are calculated together as one phase.

The overall hardness is shown in Fig. 6. It is calculated according to the equation for $HV_{average}$.

The structure and the chemical composition of the friction layer generated on the friction zone differ significantly from the bulk. The mechanical energy and generated heat contributions during braking also modify the upper zone of the bulk due to

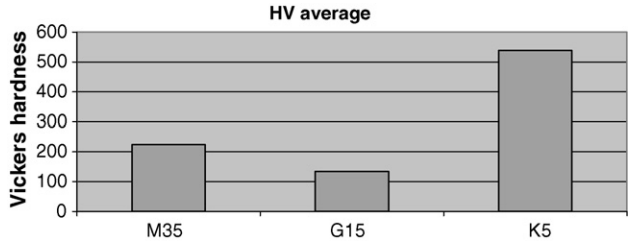

Fig. 6. The average hardness of the M35 sample and the samples with different constituent additions (G—graphite, K—SiC).

the plastic deformation of the sintered metallic constituents. The mixing of the metallic phases and their oxidation result in the formation of the friction layer. The layer contains Fe- and Cu-type oxides, with the iron oxides covered by the partially oxidized copper. During the braking we suppose that the iron-rich areas oxidized first and copper-rich phase, which is softer, spread over iron oxides and oxidized later due to the higher COF. The formation of impressed Cu/Fe oxide stripes (shown in Figs. 7 and 8) might be due to the much higher COF of the Cu-rich area locally causing hot spots on the friction surface. This leads to the formation of Fe-based oxides covered with partially oxidized copper, which are then impressed into the soft, mixed metallic matrix. This should be proven by additional experiments with lower number of braking during friction test.

The addition of SiC and graphite to the base metallic matrix M35 has a strong influence on friction-layer formation. Abrasive particles suppress sintering and movement of the metallic phases, and the upper part close to the surface of the lining which is not so well sintered and dense. The friction layer is thinner and discontinuous (Fig. 5—K5). Graphite (G15) has a minor influence on friction-layer formation, but it has a strong effect on the hardness of the pad (Fig. 6). Friction layer is present and has similar structure and thickness as M35 with the high discontinuously due to the more than 40 vol.% of graphite phase in G15 lining. In spite of it being a lubricant the addition of

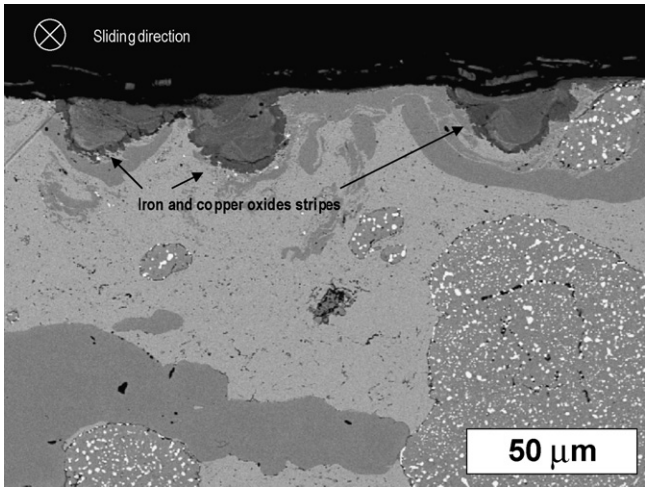

Fig. 7. SEM micrograph of a cross-section of the M35 sample showing the mixed metallic matrix with impressed iron and copper oxide stripes forming the friction layer. The disc's sliding direction is perpendicular to the picture area.

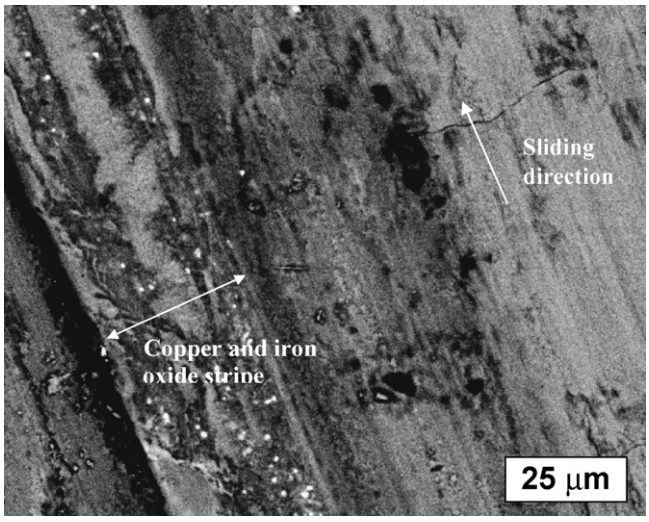

Fig. 8. SEM micrograph of sliding surface of M35 sample showing part of the iron and copper oxides stripe with V, W carbide precipitates from the HSS phase (white spots).

graphite to M35 raises the COF, which can be explained by the softer pad material: the softer the material, the larger the actual contact area, and the higher the COF.

4. Conclusions

- We found that the friction performance of MMC-type bake pads on a C/C–SiC brake disc is dependent on the base metallic matrix composition and formation of a friction layer on the brake pad surface.
- The structure and the chemical composition of the friction layer generated on the friction surface are significantly different to that of the bulk.
- Mechanical energy and generated heat contributions during braking also modify the upper part of the lining due to plastic deformation and additional sintering of the sintered metallic ingredients.
- Mixing of the metallic phases and their oxidation generated the formation of a friction layer. We observed that it is composed of Fe- and Cu-type oxides, and that the iron oxides were mostly covered with the partially oxidized copper.
- Abrasive particles (SiC) suppress the displacement of metallic phases, and the upper matrix was not completely sintered and so it was less dense. The friction layer was thinner and not continuous. The material also shows a lower mean COF.
- Graphite has a minor influence on the formation of the friction layer but it has a strong effect on the hardness of the pad. Although it is a lubricant the addition of graphite to M35 raised the COF, presumably by reducing its hardness, which can be explained by the softer pad material: the softer the material, the larger the actual contact area and the higher the COF.

References

1. Savage, G., Applications of carbon–carbon composites. *Carbon–Carbon Composites* (*1st ed.*). Chapman & Hall, London, 1993, pp. 323–346.

2. Krupka, M. and Kienzle, A., Fiber reinforced ceramic composite for brake discs. *Proceedings of the 18th Annual Brake Colloquium and Engineering Display*. SAE Paper No. 2000-01-2761, SAE, Warrendale, 2000, p 358.
3. Heine, M. and Gruber, U., Silicon carbide articles reinforced with short graphite fibers. U.S. Patent 6 030 913, 29 February 2000.
4. Zornik, M., Brake/clutch disc, such as for a vehicle. U.S. Patent 6 077 607, 20 June 2000.
5. Gern, H. and Kochendörfer, R., Liquid silicon infiltration: description of infiltration dynamics and carbide formation. *Composites Part A*, 1997, **28A**, 355–364.
6. Hilling, W. B., Making ceramic composites by melt infiltration. *American Ceramic Society Bulletin*, 1994, **73**, 56–62.
7. Stadler, Z., Kermc, M., Kosmac, T. and Dakskobler, A., A motorcycle brake system with C/C–SiC composite brake discs. In *28th International Conference on Advanced Ceramics and Composites, Cocoa Beach, Florida. Ceramic Engineering & Science Proceedings*, ed. Lara-Curzio, E. and Readey, M. American Ceramic Society, Westerville, 2004, **25** (4) 179–184.
8. Eriksson, M. and Jakobson, S., Tribological surface of organic brake pads. *Tribology International*, 2000, **33**, 817–827.
9. Filip, P., Weiss, Z. and Rafaja, D., On friction layer formation in polymer matrix composite material for brake application. *Wear*, 2002, **252**, 189–198.
10. Österle, W. and Urban, I., Friction layers and friction films on PMC brake pads. *Wear*, 2004, **257**(1–2), 215–226.
11. ECE Regulation No. 90, Annex. 8. Determination of friction behaviour by machine testing.
12. Pedersen, L. M., The effect of graphite in sintered friction materials. Industrial Ph.D. Thesis. Materials Technology Department of Engineering, The Technical University of Denmark, 2001.
13. Kermc, M., Stadler, Z. and Kalin, M., Surface temperatures in the contacts with steel and C/C–SiC—composite brake discs. *Journal of Mechanical Engineering*, 2004, **50**(7/8), 348–359.
14. Kermc, M., Kalin, M. and Vizintin, J., Development and use an apparatus for tribological evaluation of ceramic-based brake materials. *Wear*, 2005, **259**, 1079–1087.
15. Stadler, Z. and Secnik, S., Friction material and manufacturing thereof. PCT WO2004/081405 A1, 23 September 2004.
16. Gmelins Hanbuch der Anorganischen Chemie. Kohlenstoff, Teil B-Lieferung 2, *Vol 14*, 8th ed., Verlag Chemie GMBH Weinheim/Bergstr., 1968.